V.P. EFREMOV*, A.A. FROLOV*, E.M. DIANOV**, I.A. BUFETOV**, V.E. FORTOV*

DYNAMICS OF LASER-INDUCED SHOCK WAVE IN SILICA

DYNAMIKA LASEROWA INDUKOWANA W FALI UDERZENIOWEJ W KRZEMIONCE

The studyof detonation-like mode of laser induced damage propagation was considered. Velocity of this propagation is two orders of magnitude faster than known published data on burning fiber glass. The condition of optical fiber and enough long laser pulse let us obtain laser induced damage propagation passing near hundred own core diameters during pulse. The using as target the core of silica-based optical fiber has some diagnostic advantages. It allows spatially splits "start" and "stop" points and to supply the same form of energy deposition in every cross section of optical fiber. Tested regime demonstrates near constant velocities during 250 ns in the range of laser intensity 2-4.5 GW/cm^2.

Keywords: laser supported detonation, silica-based optical fiber, laser induced damage

W pracy analizowano detonacyjny typ laserowo indukowanej propagacji zniszczenia. Stwierdzono, że prędkość tej propagacji jest dwa rzędy wielkości większa aniżeli ta, która jest zawarta w dostępnych danych literaturowych dla spalania włókien szklanych. Stan włókna szklanego oraz wystarczająco długi impuls lasera prowadzą do osiągnięcia laserowo indukowanej propagacji zniszczenia przekraczającego ok. 100 średnic rdzenia włókna podczas jednego impulsu. Zastosowanie, jako obiektu rdzenia, krzemionkowego włókna szklanego ma szczególną korzyść diagnostyczną. Mianowicie, umożliwia przestrzenne rozdzielenie punktu „staru" i „stopu" oraz zapewnia tę samą formę energii „uwolnionej" na każdy przekrój poprzeczny włókna optycznego. Zastosowane zakresy testów pokazują naw przybliżeniu stałe prędkości propagacji zniszczenia w okresie 250 ns, dla zakresu intensywności wiązki lasera 2-4.5 GW/cm^2.

1. Introduction

Hydrodynamics of laser induced damage in transparent dielectrics is rather complex physical event [1, 2]. This event is determinated by the variety of parameters (laser intensity, pulse length, photon energy and band-gap value). Evolution of laser damage from initiation (loss of transparency) to material fracture is governed by energy deposition dynamics and material properties. Prominent role among transparent dielectrics belongs to silicon dioxide. In particular silica is one of the main working media for powerful optical fiber lasers.

However the silica properties present difficulties at describing. For example the high melting temperature of silica is a serious challenge to experiments with the liquid at elevated pressure. Historically available data have been inferred either to glasses at high pressure or to liquids at low pressure. Also it is rather complicated the silica properties under moderate pressures and temperatures where silica is nonlinear elastic material and there is thermally activated densification resulted from irreversible transformation of glass network [3]. High pressures up to ~10 TPa and temperatures up to 10^5 K can be achieved inside transparent dielectrics in laser-induced damage experiments [4].

There are different ways for inducing the changes in a bulk solid by laser action. First, reversible material loading can be induced by lasers at the intensity below the damage threshold. Second, irreversible structural changes may be produced at high intensity above the optical breakdown threshold, when strongly absorbing plasma occurs in a small volume of the bulk and produces a fast energy release. As a result a strong shock wave is generated and it propagates into the surrounding cold material. The shock wave propagation is accompanied by compression of the solid material at the front and rarefaction behind it leading to the formation of a void with cracks around it.

If an optical absorption coefficient is strongly increased during pressure pulse third way becomes possible [5] even under subthreshold laser intensities. This way of destruction core is laser supported detonation (LSD) which propagates under subthreshold intensities. We are assuming that in this case the damage propagation is driven by high pressure hydrodynamics. LSD model should be distinguished from the moving breakdown one where there is an ionization front propagation during the laser pulse in the focused laser beam [6]. Nevertheless silica is everywhere used in different constructions under extreme conditions. In particular silica is one of the main working media for powerful optical fiber lasers.

*   JOINT INSTITUTE FOR HIGH TEMPERATURES RAS, RUSSIA, 125412, MOSCOW, IZHORSKAYA 13/2

**   FIBER OPTICS RESEARCH CENTER RAS, 119333, MOSCOW

New object of laser damage manifestation is the core of silica-based optical fibers [7, 8]. And study of such bulk damage becomes rather significant due to world progress in optical communication link application.

In the previous work we had reported the observation of laser-induced damage wave propagated with the velocity ~3km/s through the optical fiber core [8]. We have used single mode optical fibers. In these fibers the laser intensity distribution is constant at every cross-section along the full length of fiber (a mode field diameter (MFD) is the $1/e^2$ width of this distribution). This property supplies observing wave under steady-state conditions. While another works had used with the focused laser beam only. This is especially important in the case of long laser pulses ($t_p > 1$ns) when hydrodynamic gives a significant effect on of plasma propagation distance (comparable with core diameter in our case). In the present paper we continue the analyzing of process details.

2. Measurement techniques and results

We had tested three types of silica-based optical fibers. Parameters of these fibers are described in Table 1. (Types of used fibers and corresponding photo: Fig. 2 – (F1), Fig. 3 – (F3, top) (F1, bottom), Fig. 4 – (F2), Fig. 7 – (F3), Fig. 8 – (F2, top) (F3, bottom)). Energy distributions in core for different fibers are shown in Fig. 1.

TABLE 1

Parameters of silica-based optical fibers. For fiber F2 with a big central dip in the refractive index profile RID is the value for the effective step-index profile; the fiber F3 is Corning SMF-28^{TM}

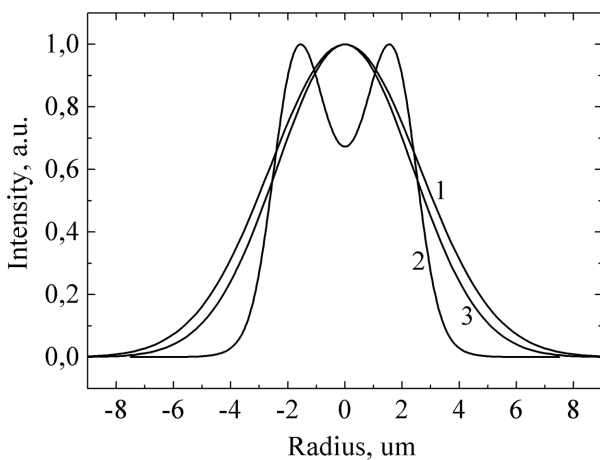| Name of fiber	F1	F2	F3
Silica cladding diameter, um	600	125	125
Core diameter, um	9.5	7.7	8.2
Refractive index difference (RID)	0.006	0.013	0.005
Composition SiO$_2$:GeO$_2$:Al$_2$O$_3$	97:1:2	89:11:0	96.5:3.5:0
Mode field diameter at 1064 nm, um	10.5	6.13	8.9

Fig. 1. The intensity distributions of the laser radiation in the optical fibers: 1 corresponds to fiber (F1), 2 – (F2), 3 – (F3)

As in the our previous work [7, 8] driving laser pulses were supplied by Nd3$^+$:YAG laser (λ =1.064um) in Q-switched mode with 5 kHz repetition frequency. Temporal intensity profile was near-Gaussian shape (with FWHM of ~250ns) with a peak intensity of 4-4.5 GW/cm^2 in the fiber core. To initiate LSD free exit of the optical fiber was touched by a metal absorption surface. LSD had started to move when the laser intensity became greater than ~2GW/cm^2 with the velocity around 3 km/s. The distance of this wave propagation was around ~400-700um per pulse.

Photo of fiber after LSD propagation is shown in Fig. 2. Relation between the damage tracks and the laser pulses is presented at lower graph in Fig. 2. That is process is moving during the part of laser pulse. Next laser pulse initiated new LSD near point of previous stopping.
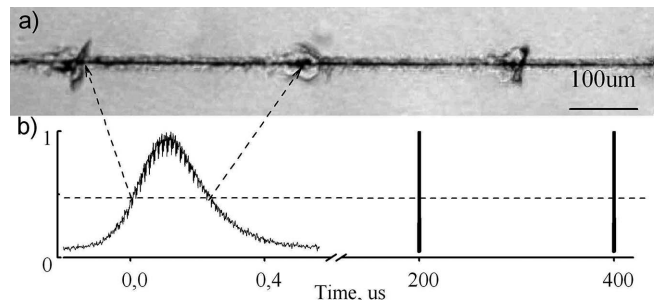
Fig. 2. The damage track in optical fiber under the laser pulse train: a) the micrograph of the damaged F1, b) the temporal dependence of the laser intensity (in arbitrary units). The laser radiation propagated from right to left
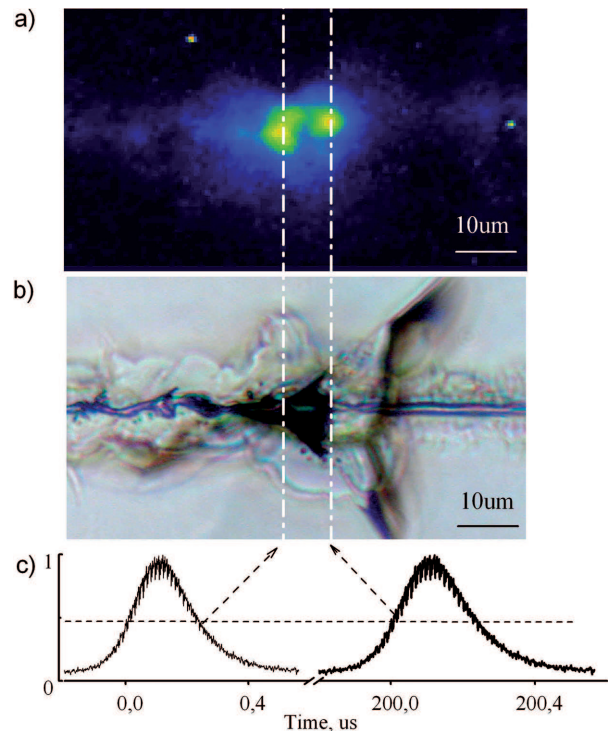
Fig. 3. The micrographs of the region with the start and stop points: a) the plasma glow during damaging (the 1s exposure time), b) the failure picture after process, c) the temporal dependence of the laser intensity (in arbitrary units)

Fig. 3 exhibits more details the region of Start and Stop (S&S) points. The immobile plasma glows during Start and Stop points (See Fig 3a). Core heating at these moments is supplied by laser pulse tails below threshold intensity. Failure

picture after process is shown in Fig 3(b). S&S distance is about 8.3um. Most likely this distance is determined by heat wave propagation between laser pulses.
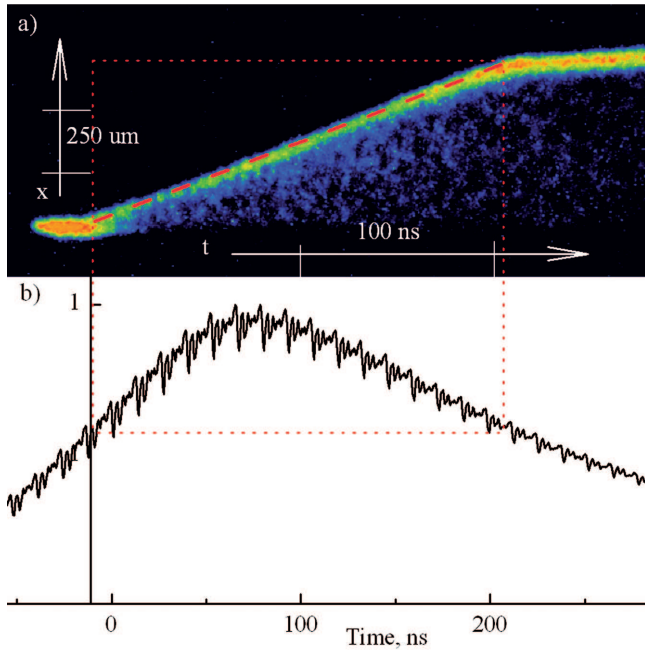

Fig. 4. The plasma propagation in the fiber core under laser pulse: a) the streak camera image, b) the oscilloscope picture of the laser intensity (in arbitrary units). The red dashed line has been laid throughout the maximums of plasma glow

For velocity measuring we have used the streak camera with microscope objective. The streak camera image of plasma propagation (the frame sizes of 1mm×350ns) and the oscilloscope picture of the laser intensity are shown in Fig. 4. The red dashed line has been laid throughout the maximums of plasma glow. We had observed very short time of acceleration not more than 1-1.5 core diameters and then velocity stabilizes.

Distances of propagation LSD as function of time motion are presented in Fig. 5 for fibers F1 and F2. (Number in circles correspond to number of fiber)
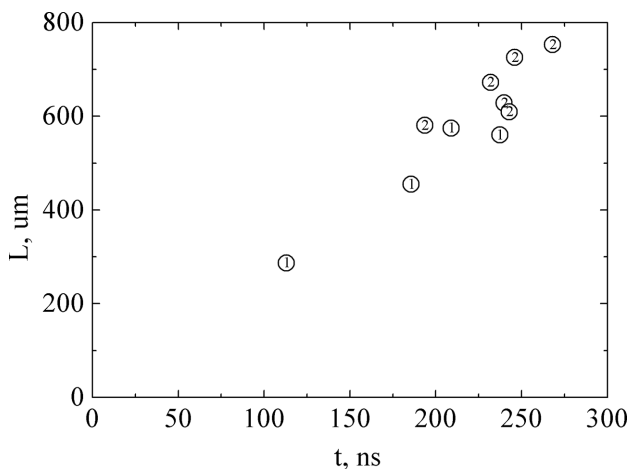

Fig. 5. The traveled distance of LSD vs. the motion time

Data on the absorbing front velocity as a function of average energy intensity are presented in Fig. 6. Velocity is slightly increasing with average dissipated laser energy.
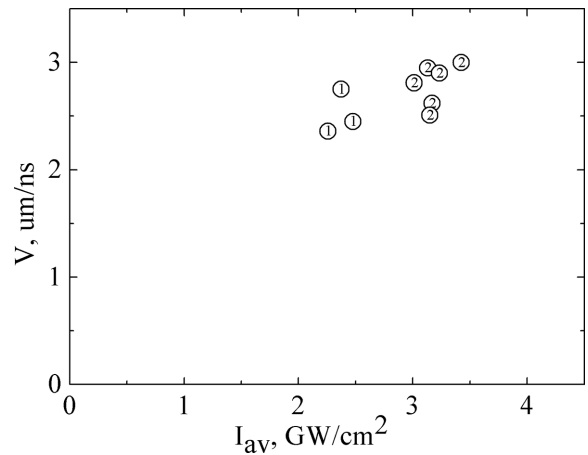

Fig. 6. The dependence of the LSD velocity vs. the average laser intensity during LSD

Micrographs had been obtained for fiber F3 (These fibers were doped with GeO_2 and had MFD of 9um.) (Corning SMF-28, GeO_2 mol. concentrations of 4%). A silica cladding of the fibers had the diameter of 125um.

An optoelectronic camera (Nanogate-3n, NPP Nanoscan with S-1 photocathode sensitive to a visible light) with microscope objective (with 10×magnification) we have to obtain micrograph images. A minimum exposure time was 2ns. As backlight the beam of second-harmonic generation (532nm) from the driving laser has been applied. An image was projected onto the camera photocathode by a selective dielectric mirror mounted at an angle of 45 degrees. The mirror had the reflectivity of 55% at 530 nm under normal incidence.

To make clear LSD features we had applied three types of technique for obtaining images. There were a bright field microscopy for crack formation, thermal emission for plasma zone visualization and a stress-induced birefringence through the crossed polarizers for pressure pulse.

The photo in Fig. 7 (left) demonstrate the plasma zone glow. Relative blackening along fiber axis represents line 1 in Fig. 7 (right) across fiber axis represents line 2 in Fig. 7 (right)
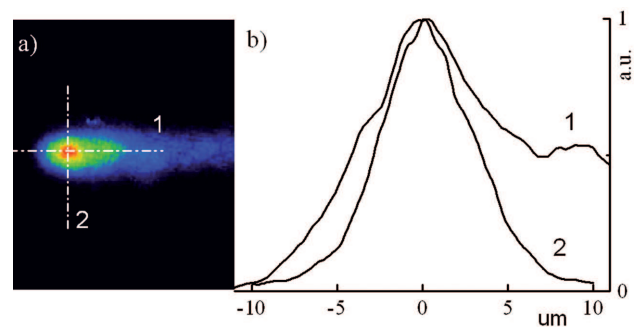

Fig. 7. The high-speed micrography of the laser plasma in the core of F3: a) the 2ns exposure time micrograph of the plasma propagated from right to left with speed of 2.8um/ns, b) the glow intensity curves

The micrograph image in Fig. 8a demonstrates the initiation and formation of individual cracks ahead of the plasma front. The cracks are separated by the distance of ~2-3 um. They begin on the core-cladding interface and propagate almost radially outwards. The plasma temperature under our conditions is around 10^4K [9]. This correlates with measure-

ments in [10]. In this work plasma broadband emission was found to have a Planckian distribution throughout the entire lifetime and achieved plasma temperature was 10.5kK around a threshold breakdown condition. The spatial distribution of a wave emission is shown in Fig. 4 (right). One can see that the high temperature domain has a rather small size therefore there is motion blur in the longitudinal direction due to the plasma front propagation during the exposure time of the camera. At the same time we see distinguishly more immobile cracks in Fig. 8a.
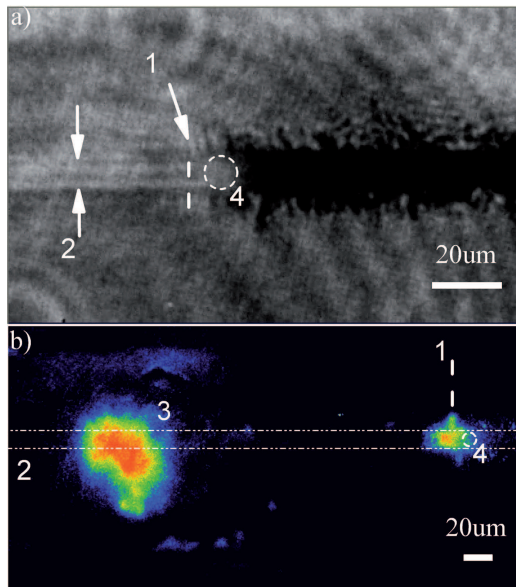

Fig. 8. The high-speed micrography of LSD (the 2ns exposure time): a) shadow picture, b) in-crossed-polarizers picture. 1 – the cross-section plane of the radial crack appearance (dash line), 2 – the fiber core, 3 – the solitary stress wave, 4 – the laser plasma (dotted circle)

To get the inherent longitudinal profile of the emission we have examined a digital convolution of the transversal profile passed through a maximum of the emission and the instrumental function (for the 1.8ns-time window and the object velocity of 2.8um/ns). In high temperature region the convolution curve agrees well with the profile on the front side of the micrograph image Fig.7 (right). Thus the plasma zone had a nearly spherical shape. In front of plasma zone there is a shoulder in the longitudinal profile, where the brightness exceeds the mount of thermal emission of the plasma. It is an important feature to understand LSD in optical fibers.

Stress-induced birefringence is used to measure axial stresses in optical fibers [11, 12]. We applied optical microscopy between crossed polarizers to examine stresses arising in the fiber at LSD. A longitudinal pressure wave (precursor) in the silica cladding and fiber core propagates before the plasma front. Plasma zone wave were observed as light regions where a stress-induced birefringence rotates a plane of the light polarization (Fig. 8b). In shock wave a stress distribution is bell-shaped without a rarefaction region and the wave occupies all the fiber in diameter. On the other hand, in plasma front a strain localized region is in the fiber core where a GeO_2:SiO_2 glass with a lower elastic modulus than in silica cladding. The position of radial crack formation was observed also in this method. It is possible to properly combine the

images obtained by different techniques. Optical absorption, light scattering and plasma fluorescence complicate the interpretation of the obtained pictures. We could estimate the values of longitudinal compressive stress due to birefringence fringes observed in stress wave (SW) region. In the linear approximation with optic-stress coefficient $35.5?10^{-13} Pa^{-1}$ [12] the compressive axial stress of the core in the crack formation plane was ~4GPa and the maximum of SW was ~2GPa. If the pressure linearly increases in the plasma front the plasma pressure would be evaluated as around 8-10 GPa.

3. Discussion

Our measurements had visualized new details of detonation like process of destruction of silica-based optical fibers. Is the concept of detonation applicable here? Detonation model assumes that absorption of laser radiation in material begins as a result of hydrodynamic processes induced by energy deposition in laser plasma. If the propagation velocity was greater than sound speed usage of the model would be apparent. Now we have some deviations from ideal detonation. Obtained regime has curved front (not flat), propagation velocity less than sound velocity in pure silica and structure of front is complex. Front of oobtained regime demonstrates two wave structure (plasma zone and precursor). In addition silica properties under loading are rather complicated what creates difficulties in the interpretation. Processes of optical absorption increasing are strongly depended on pressure and temperature [13-20]. A laser heating of silica by infra-red radiation is determinated by an optical absorption of free electrons in conduction band [13]. A dramatic increase of optical absorption has been shown in the shock heating of silica [14] which resulted from the rapid increase electrical conductivity linked with the dissociation of Si-O bonds [15] for pressures larger than 70 GPa. But in case of laser breakdown in bulk of silica at a few ns pulse there is strongly localized plasma with pressure of ~25-30 GPa only [10]. The plasma pressure modifies the surrounding material to become absorbing [16]. Contribution of hydrodynamic motion we can see in experiments of work [17]. In our case the absorption may be connected with a thermally activated glass network transformation resulting in a permanent glass compaction under pressure below 10GPa [1]. A compaction leads to the appearance of slow shock wave with the velocity of 3km/s just above the elastic limit (the particle velocity of 1 km/s) like in a flyer plate experiment in work [18]. The core glass should be compressed and compacted by pressure from laser plasma. It is accompanied by changes in glass network and increasing the number of overcoordinated silicon atoms. Rigid structure domains are formed around these silicon atoms. Apparently when "rigid clusters" form a rigid network (rigidity percolation) breaking and rebounding of chemical bonds dramatically increase [19]. After the onset of LSD we observed a threefold decrease of laser plasma brightness. This may be explained due to self-trapped exciton (STE) absorption of visible radiation from the laser plasma because of energy states of STE changed under relaxation of Si-O bond [20]. Therefore STEs would be excited in the triplet state T1 in the shock wave front. And a subsequent ionization of the exited STEs apparently is necessary to generate

of free electrons which are responsible for laser heating of SiO_2 at 1.064um. Besides processes mentioned above the rarefaction wave action should be taken into account. Review of mechanism of loss transparency is presented in work [21]. It's necessary to note that we had investigated core of fiber consisted of SiO_2 with additives (See Table 1) meanwhile most of available data are mainly correspond to pure silica. The question of detonation model applicability remains open still and demands new experiments.

4. Conclusions

Investigation of detonation-like mode of laser induced damage propagation detected in our early work [8] has been continued in this study. This propagation regime is two orders of magnitude faster than known published data on burning fiber glass. The condition of optical fiber and enough long laser pulse let us obtain laser induced damage propagation passing near hundred own core diameters during pulse. The using as target the core of silica-based optical fiber has some diagnostic advantages in comparison with approaches developed in works [1, 2].

At least it allows spatially splits "start" and "stop" points and to supply the same form of energy deposition in every cross section of optical fiber. Tested regime demonstrates near constant velocities during 250ns. Observed velocity stationarity in our experimental conditions (2-4.5 GW/cm^2) is rather unexpected result.

Recorded photo of front structure of failure and plasma waves in a core of silica-based optical fiber shows distinguishly cracks directly starting from plasma and pressure wave. Exposure time was 2ns. Heating rate in the front of plasma wave was $\sim 4 \times 10^{12}$ K/s. Application of optical technique with crossed polarizers makes it possible to visualize of pressure pulse. In our opinion pressure zone creates the destruction area where starts particle losing of transparency. It means moving laser absorption front and plasma region. In this case velocity of process is limited by failure wave velocity. For higher laser intensity, laser absorption front will be located directly after shock front. Though dominating mechanism of the transparency loss at pressure wave demands additive investigations. This work has been done due to support Presidium RAS Program.

REFERENCES

[1] G. D u c h a t e a u, M.D. F e i t, and S.G. D e m o s, J.Appl.Phys. **111**, 093106 (2012).

[2] C.W. C a r r, J.D. B u d e, and P. D e M a n g e, Phys. Rev. B **82**, 184304 (2010).

[3] Y. I n a m u r a, Y. K a t a y a m a, and W. U t s u m i, J. Phys. Condens. Matter. **19**, 415104 (2007).

[4] L. H a l l o, C. M e z e l, A. B o u r g e a d e, D. H e b e r t, E.G. G a m a l y, NATO Science for Peace and Security Series B: Physics and Biophysics, Extreme Photonics & Applications, 121 (2010).

[5] M. v o n A l l m e n, and A. B l a t t e r, Laser-Beam Interactions with Materials: Physical Principles and Applications. Springer. 2002. 2nd edition.

[6] F. D o c c h i o, P. R e g o n d i, M.R.C. C a p o n, and J. M e l l e r i o, Appl. Opt. **27**, 17, 3661 (1988).

[7] E.M. D i a n o v, V.E. F o r t o v, I.A. B u f e t o v, V.P. E f r e m o v, A.E. R a k i t i n, M.A. M e l k u m o v, M.I. K u l i s h, A.A. F r o l o v, Optical Communication, 2005. ECOC 2005. 31st European Conference 25-29 Sept., **3**, 469 (2005).

[8] E.M. D i a n o v, V.E. F o r t o v, I.A. B u f e t o v, V.P. E f r e m o v, A.A. F r o l o v, M.Y. S c h e l e v, and V.I. L o z o v o i, J. Exp. Theo. Phys. Lett. **83**, 2, 75 2006.

[9] V.P. E f r e m o v, E.M. D i a n o v, V.E. F o r t o v, I.A. B u f e t o v, A.A. F r o l o v, Physics of Extreme States of Matter. Chernogolovka, 41 (2011).

[10] C.W. C a r r, H.B. R a d o u s k y, A.M. R u b e n c h i k, M.D. F e i t, and S.G. D e m o s, Phys. Rev. Lett. **92**, 8, 087401 (2004).

[11] M.J. S a u n d e r s, Rev. Sci. Instrum. **47**, 4, 496 (1976).

[12] P.L. C h u, and T. W h i t b r e a d, Appl. Opt. **21**, 23, 4241 (1982).

[13] X.A. S h e n, S.C. J o n e s, and P. B r a u n l i c h, Phys.Rev.Lett. **62**, 23, 2711 (1989).

[14] D.G. H i c k s, T.R. B o e h l y, J.H. E g g e r t, J.E. M i l l e r, P.M. C e l l i e r s, and G.W. C o l l i n s, Phys. Rev. Lett. **97**, 025502 (2006).

[15] J. C l e r o u i n, Y. L a u d e r n e t, V. R e c o u l e s, J.Phys.A: Math. Gen. **39**, 4387 (2006).

[16] R.A. N e g r e s, M.D. F e i t, P. D e M a n g e, J.D. B u d e, and S.G. D e m o s, Proc. of SPIE. **6720**, 672019 (2007).

[17] R.A. N e g r e s, M.D. F e i t, and S.G. D e m o s, Opt. Express. **18**, 10, 10643 (2010).

[18] A. K u b o t a, M.-J. C a t u r l a, J.S. S t ö l k e n, M.D. F e i t, Opt. Express. **8**, 11, 611 (2001).

[19] K. T r a c h e n k o, and M.T. D o v e, Phys. Rev. B **67**, 212203 (2003).

[20] S. I s m a i l - B e i g i, and S.G. L o u i e, Phys. Rev. Lett. **95**, 156401 (2005).

[21] A. K u s o v, A. K o n d y r e v, and A. C h m e l, J. Phys.: Condens. Matter. **2**, 4067 (1990).